Biochemical Pharmacology, Vol. 60, pp. 963–967, 2000.

ISSN 0006-2952/00/$–see front matter
PII S0006-2952(00)00421-4

SHORT COMMUNICATION

Validation of Fluorouracil Metabolite Analysis in Excised Tumor

LABILITY OF ANABOLITES

James R. Bading,† Antranik H. Shahinian,* Melanie T. Paff,‡ Paul B. Yoo* and David W. Hsia**

*Department of Radiology, University of Southern California, Los Angeles, CA; ‡Division of Bioanalysis and Drug Metabolism, Glaxo Wellcome, Inc., Research Triangle Park, NC, U.S.A.

ABSTRACT. Rapid excision and freezing of tissue commonly is assumed to preserve the molecular composition of the tissue just prior to its removal from the host. We examined the lability of radiolabeled 5-fluorouracil (FUra) and its anabolites during excision and freeze-clamping in a rat tumor model. Acid-soluble metabolites were identified by HPLC. Two rats, each bearing multiple, subcutaneously-implanted colon tumors, were treated with eniluracil (an inactivator of dihydropyrimidine dehydrogenase) to prevent catabolism of FUra and then injected intravenously with [^{3}H]FUra. After 2 hr, tumors were harvested sequentially and segmented. The tumor pieces were kept at room temperature for various times up to 4 min prior to freezing. These specimens showed a decrease ($P < 0.01$) in labeled nucleoside triphosphate content of 13 ± 2%/min and commensurate increases ($P < 0.005$) in labeled nucleoside monophosphates and nucleosides with increasing time-to-freeze. The amounts of labeled macromolecules, nucleoside diphosphates, and FUra each remained approximately constant. The study indicates that substantial errors may occur in measured tissue concentrations of pyrimidine nucleosides and nucleotides due to lability during tissue excision and freeze-clamping. Such errors can be corrected using data of the type obtained in this study. BIOCHEM PHARMACOL **60**;7:963–967, 2000. © 2000 Elsevier Science Inc.

KEY WORDS. antimetabolites; pyrimidines; fluorouracil; adenocarcinoma; metabolism; biological assay

It is common practice to perform biochemical analysis on tumor or normal tissue that has been removed from human patients or laboratory animals and quickly frozen to arrest metabolic activity. However, the literature contains little information about molecular lability during the period between the start of tissue excision and the completion of the freezing process. We faced this problem in connection with a study of the anabolic kinetics of FUra§ in a rat colon tumor model. We were seeking to develop a technique for non-invasive measurement of FUra kinetics in tumors using PET and [^{18}F]FUra [1], and we wanted to validate the PET measurements by comparison with direct, *ex vivo* metabolite assays. Thus, it was necessary to assess the absolute accuracy of the *ex vivo* procedure, i.e. to quantify any changes in the molecular distribution of the radiolabel between the end of the PET study (coincident with the start of tumor excision) and the completion of the metabolite analysis procedure (i.e. tissue preparation, acid extraction, and HPLC of the acid-soluble extract). The frozen tumors were kept near liquid nitrogen temperature as they were ground into a fine powder and then slowly thawed in the presence of highly concentrated PCA. Not surprisingly, lability from the beginning of pulverization through the HPLC run was shown to be negligible. The remaining problem, and the subject of this paper, was to determine the change in labeled FUra and its metabolites during excision and freeze-clamping of tumors.

MATERIALS AND METHODS

Chemicals

Eniluracil (5-ethynyluracil, Glaxo Wellcome compound 776C85) was supplied under special agreement by Glaxo Wellcome, Inc. Tritium-labeled 5-fluorouracil ([6-^{3}H]FUra, 20 Ci/mmol, radiochemical purity >98%) was purchased from Moravek Biochemicals. Non-radiolabeled chemicals used as references for identification of radiolabeled chromatographic peaks were purchased from the Sigma Chemical Co. with chemical purities as indicated in the following list: FUra (≥99%), FUrd (≥99%), 5-fluoro-2′-deoxyuridine (FdUrd, ≥99%), 5-fluoro-2′-deoxyuridine monophosphate (FdUMP, 85%), UDP (96%), and UTP (97%). FUMP (>99%), 5-FUTP (>97%), and FdUTP (>97%)

† Corresponding author: James Bading, Ph.D., PET Imaging, 1510 San Pablo St, Suite 350, Los Angeles, CA 90033-4609. Tel. (323) 342-3254; FAX (323) 342-3253; E-mail jbading@hsc.usc.edu.

§ *Abbreviations*: AIF, acid-insoluble fraction; ASF, acid-soluble fraction; DPD, dihydropyrimidine dehydrogenase; FUra, 5-fluorouracil; FUrd, 5-fluorouridine; FdUrd, 5-fluoro-2′-deoxyuridine; FUMP, 5-fluorouridine monophosphate; FdUMP, 5-fluoro-2′-deoxyuridine monophosphate; FUDP, 5-fluorouridine diphosphate; FdUDP, 5-fluoro-2′-deoxyuridine diphosphate; FUTP, 5-fluorouridine triphosphate; FdUTP, 5-fluoro-2′-deoxyuridine triphosphate; PCA, perchloric acid; and PET, positron emission tomography.

Received 7 January 2000; accepted 30 March 2000.

were obtained as special preparations from Sierra Bioresearch. Liquid scintillation fluid (RIA-Solve II) was purchased from Research Products International.

Tumor Model

Experiments were conducted with a rat colorectal tumor (Ward tumor) grown in Fischer-344 albino rats [2]. The response of the Ward tumor to FUra is very similar to that of human colorectal carcinoma, and the tumor has been used to study the effects of a number of different biochemical modulations of FUra [3–5]. When implanted subcutaneously, the tumor derives its blood supply from the skin and grows in a well-encapsulated manner, i.e. not invading underlying normal tissues. Central necrosis begins to appear when the tumors reach about 1 g.

Measurement of Molecular Lability in Excised Tumor

Female Fischer-344 rats (6–7 weeks old, 180–200 g) were implanted subcutaneously by trochar injection with several small pieces (approximately 1 mm^3 each) of previously frozen tumor. Experiments were conducted when the tumors reached 1–2 cm diameter. All *in vivo* procedures were performed under anesthesia [ketamine (80 mg/kg) and xylazine (5 mg/kg) given i.p.] and conformed to a protocol approved by the Animal Care and Use Committee at our institution.

Rats were catheterized in an external jugular vein. Eniluracil (1 mg/kg i.p.) was given to prevent catabolism of FUra [3]. One hour later, [^{3}H]FUra (radioactivity dose 0.05 to 0.2 μCi/g body weight, chemical dose 2 mg/kg body weight) was injected via the catheter. The tumors were harvested sequentially between 110 and 130 min post-injection. We attempted to preserve skin-to-tumor circulation until the end of the excisions by making a relatively small cut at the base of the tumor, separating the tumor from the underlying muscle, and then severing the remaining tumor–skin connection. Following excision, each tumor was cut into three or four approximately equal parts, one of which was frozen immediately by squeezing it between blocks of dry ice. The remaining tumor pieces were kept for various times at room temperature before they were frozen. Following excision of all tumors, the rats were killed by an i.v. overdose of pentobarbital. The frozen tumor samples were stored in liquid nitrogen for subsequent metabolite analysis.

Metabolite Analysis

Samples were assayed for radioactivity by liquid scintillation counting, using the external standard method of quench correction (LS6500 counter, Beckman Instruments). Frozen tumor specimens were immersed in liquid nitrogen and PCA (5 N, 1:1 v/w of frozen specimen) and ground into a fine powder. Two hundred fifty to four hundred milligrams of the powder was thawed on ice with periodic, rapid mixing over a 10-min period. Ice-cold, deionized, distilled water was added (1.5:1 v/w), and the acid-soluble supernatant and pellet (AIF) were separated by microcentrifugation. The pellet was rinsed twice with ice-cold PCA (1 N) and assayed for radioactivity. The ASF was neutralized with 1 M potassium hydroxide, and the resulting perchlorate salt was removed by centrifugation. The fraction of total radiolabel contained in the AIF was determined from its activity and the measured activities of the rinses, salt residue, and desalted ASF.

The desalted ASF was analyzed by ion-pair HPLC using a reversed-phase, C_{18} column (4.6 × 250 mm, particle size 5 μM, Microsorb-MV, Rainin, Inc.) and multi-step, linear-gradient elution. The mobile phase was formed by mixing Solvent A [1.5 mM ammonium phosphate, 1 mM tetrabutyl ammonium phosphate (pH 3.3), 1% (v:v) acetonitrile] and Solvent B [25 mM ammonium phosphate, 1 mM tetrabutyl ammonium phosphate (pH 3.3), 30% (v:v) acetonitrile] at a combined flow of 1 mL/min according to the following schedule: 0 min, A = 100%; 15 min, A = 67%; 25 min, A = 10%; 30 min, A = 0%; 35 min, A = 0%. The column was re-equilibrated in 100% Solvent A for 60 min between sample runs. With this system, nucleobases, nucleosides, and nucleoside mono-, di-, and triphosphates were eluted as individual peaks within 35 min (Fig. 1).

Radiolabeled peaks were identified in reference to UV absorption chromatograms of a standard solution containing authentic, non-radiolabeled counterparts of the various metabolites expected in the experimental samples. Elution times differed negligibly among FUTP, FdUTP, and UTP. Hence, UTP, which is relatively inexpensive, was used in place of the fluorinated nucleoside triphosphates. Similarly, UDP was used as a standard for the fluorinated nucleoside diphosphates, since a radioactive peak coinciding with UDP was observed consistently (Fig. 1). An aliquot of the standard solution was added to the desalted ASF. Two hundred microliters of this mixture was injected onto the column, and eluant fractions (30 sec each) were collected. Measured recovery of injected ^{3}H ranged between 82 and 97% (mean 90%, SD 5%). The fraction of recovered activity associated with a given molecular species was multiplied by the percentage of total activity in the ASF to determine the overall percentage of that species in the original experimental sample. Because they were not well separated, ribonucleic and deoxyribonucleic species were not differentiated in the quantitative analysis of the chromatograms.

Data Reduction and Statistical Analysis

Radio- and UV chromatograms were plotted and analyzed to determine the distribution of radiolabel among molecular species using Microsoft EXCEL 98 (Macintosh). Time-dependence of the distribution of radiolabel among molecular species was analyzed by linear regression using EXCEL, by ANOVA using JMP, v. 3.1.5 (SAS Institute), and by

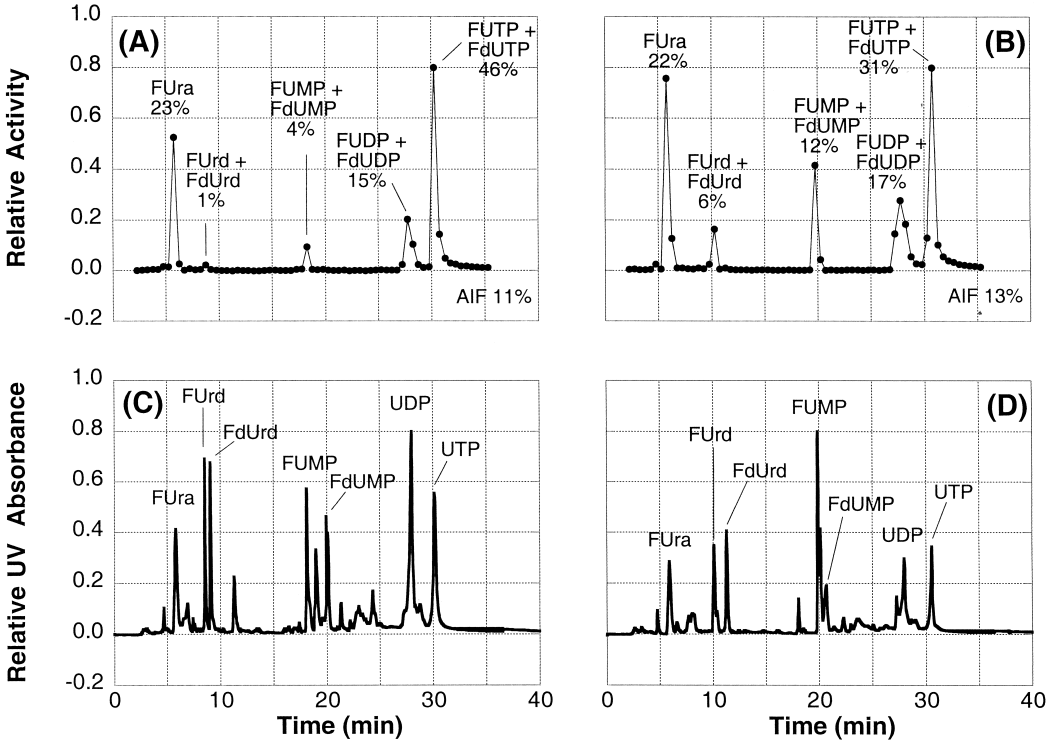

FIG. 1. Analysis of ^{3}H-labeled metabolites in Ward tumor. Shown are radiochromatograms [(A) and (B)] and corresponding UV chromatograms [(C) and (D)] obtained by gradient-elution HPLC of acid-soluble extract from two pieces of the same tumor that were frozen at different times after initiation of tumor excision. Tumors were harvested 2 hr after i.v. injection of [^{3}H]FUra from rats pretreated with eniluracil to prevent catabolism of FUra. The tumor specimen for (A) and (C) was frozen 44 sec after the start of excision, while that for (B) and (D) was frozen at 149 sec. UV absorption was measured for wavelengths =254 nm. Percentages of recovered radiolabel in each peak, as well as the AIF, are indicated in (A) and (B). Measured recovery of radioactivity injected into the HPLC system was 82% in (A) and 91% in (B). Aliquots of solutions containing authentic, non-radiolabeled samples of the compounds indicated in the UV chromatograms were added to the tumor extracts prior to injection for HPLC.

nonlinear, least-squares fitting of a compartmental model using SAAM II, v. 1.1.1 (SAAM Institute, University of Washington).

RESULTS AND DISCUSSION

Eniluracil was used to prevent *in vivo* catabolism of injected [^{3}H]FUra. This was done to increase tumor exposure to circulating [^{3}H]FUra, and hence, to increase formation of labeled FUra anabolites in tumors [1]. Eniluracil is a highly specific, mechanism-based inactivator of DPD, the enzyme that catalyzes the first step in the degradation of uracil and FUra. The compound has no antitumor activity or toxicity of its own at pharmacologic doses [6]. In principle, the use of eniluracil in our experiment may have prevented breakdown of FUra within tumor cells and/or altered the anabolic kinetics of FUra in tumors. This is unlikely, however, since DPD expression in the Ward tumor is very low relative to rat liver and intestine,* and eniluracil has a negligible effect on FUra toxicity in tumor cells with low DPD expression [7].

The experimental protocol was performed in two rats, each bearing three tumors. The data showed progressive breakdown of nucleotides to nucleosides in excised tumor tissue (Fig. 2). Time-dependence was assessed by both linear regression analysis of each data set and 2-way ANOVA (effects = rats and time) of combined data sets within each molecular species. Labeled nucleosides and nucleoside monophosphates increased with time, while nucleoside triphosphates decreased with time at a rate similar to the combined rates of increase for nucleosides and nucleoside monophosphates. No statistically significant time dependencies were observed for the AIF, nucleoside diphosphates, or FUra.

Lability was also quantified by compartmental model analysis, which had the advantage of accounting for the interdependency of the various labeled species. For each rat, a four-compartment, catenary model was fitted simultaneously to the data from each rat for nucleosides and the three nucleotide species. (FUra and the AIF were not included, since they did not change appreciably during the period of observation.) Anabolic reactions were assumed to be negligible, and the contents of the four compartments at time zero were equated with the intercepts of the respective linear regression lines. The model fits appear as curved lines in Fig. 2. Rate coefficients obtained from the compartmen-

* S. Cao, M.D., Roswell Park Cancer Center, Buffalo, NY, personal communication.

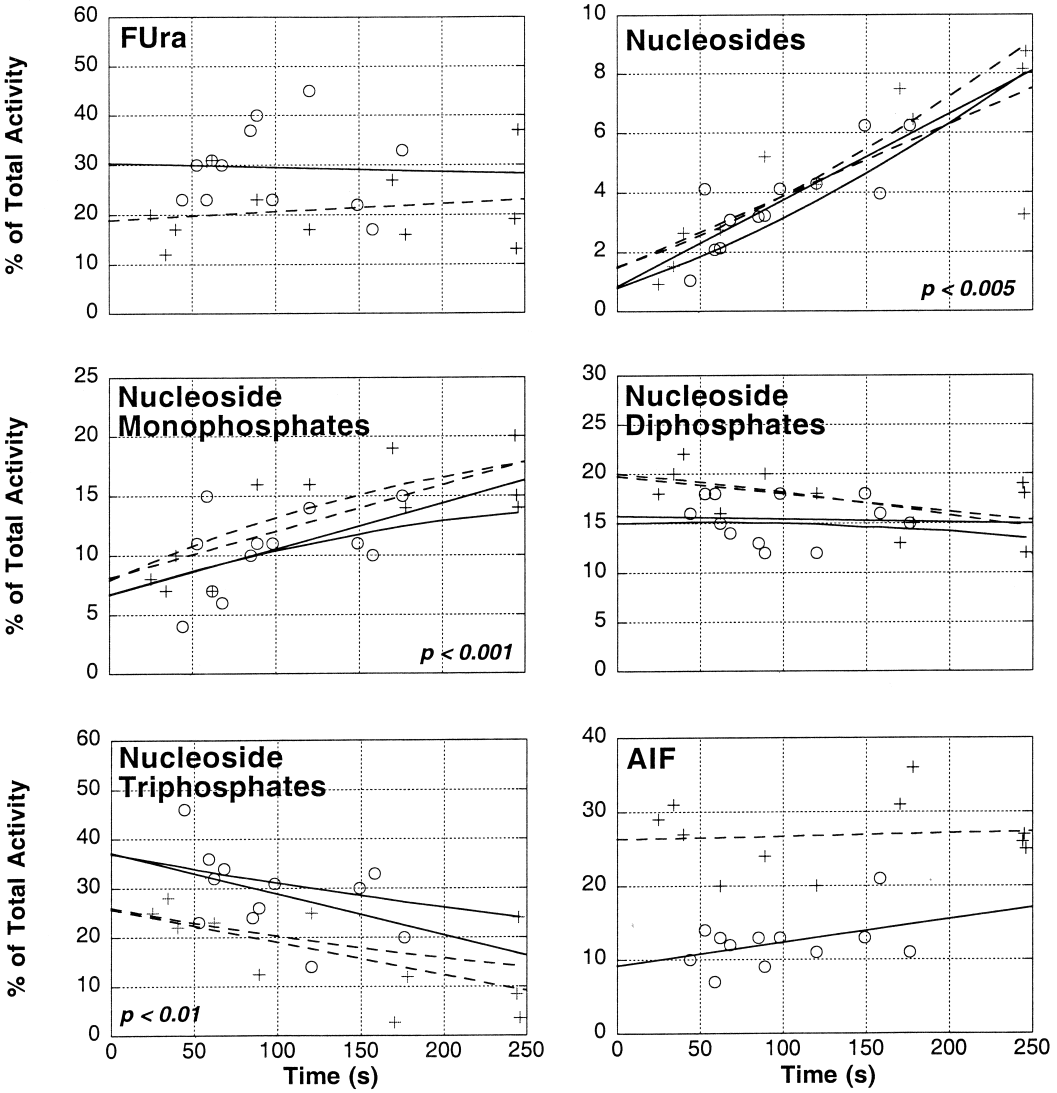

FIG. 2. Lability of ^{3}H-labeled fluorouracil and its anabolites during tumor excision and freezing. The abscissas represent the time between the start of incision and the completion of freezing. Data for each molecular species are expressed as a percentage of tumor specimen total activity, which varied between 10 and 280 nCi. (Note that the ordinate scale varies for different molecular species.) Crosses and circles denote data from two different rats. Solid and dashed lines indicate model fits to circle and cross data points, respectively. Each data set was fitted independently by linear regression (straight lines), while a compartmental model was fitted simultaneously to the data sets for nucleotides and nucleosides from a given rat (curvilinear lines). All data for each molecular species were analyzed simultaneously for time-dependence by 2-way ANOVA. The probability of constancy with time as determined by ANOVA is shown for those molecular species having a statistically significant time effect.

tal model analysis were 13 ± 2, 23.9 ± 0.1, and 15 ± 2%/min, respectively, for nucleoside tri-, di-, and monophosphates (data expressed as means ± SEM; N = 2).

Figure 2 suggests a method of correction for molecular lability during tissue excision, as follows. Analogous to the work described here, a validation study simulating the particular experimental protocol is performed, and the resulting data are fitted with a model. During the main experiments, the molecular distribution of radiolabel in tissue, and the times from start of excision to freeze, are measured. These data are used in conjunction with the model parameters obtained in the validation study to estimate the molecular distribution of the radiolabel at the start of tissue excision, or at some later time determined or assumed to mark the onset of molecular lability at the rates observed in the validation study.

A sampling of the literature reveals that investigators rarely document the accuracy of measurements of tissue metabolites obtained by the rapid-excision, freeze-clamping technique. (Examples of this for FUra can be found in Refs. 8–14.) The data reported here indicate that nucleoside triphosphates of FUra, and presumably of other pyrimidine nucleobases, may be underestimated substantially and the corresponding nucleoside monophosphates and nucleosides overestimated substantially if excision and freeze-clamping are not completed in well under 60 sec. The implication is that investigators interested in quantifying such molecules in tissue should (a) be very careful to minimize the period

of potential ischemia, (b) measure molecular lability during excision and freezing for the compounds and tissues with which they are working, and (c) if necessary, estimate and correct for molecular lability during tissue excision.

This work was funded in part by the James H. Zumberge Faculty Research and Innovation Fund, University of Southern California. Eniluracil used in this study was a gift from Glaxo Wellcome, Inc., through Dr. Thomas Spector. The procedure for preparing and analyzing tissue for FUra and its metabolites was developed at Glaxo Wellcome. The Ward tumor was provided by Dr. Youcef Rustum, Sr. Vice President for Scientific Affairs, Roswell Park Cancer Institute.

References

1. Bading JR, Alauddin MM, Fissekis JH, Kirkman E, Raman RK and Conti PS, Blocking catabolism enhances PET studies of 5-[F-18]fluorouracil pharmacokinetics. *J Nucl Med* **38:** 176P, 1997.
2. Rustum YM, Toxicity and antitumor activity of 5-fluorouracil in combination with leucovorin. Role of dose schedule and route of administration of leucovorin. *Cancer* **63:** 1013–1017, 1989.
3. Cao S, Rustum YM and Spector T, 5-Ethynyluracil (776C85), Modulation of 5-fluorouracil efficacy and therapeutic index in rats bearing advanced colorectal carcinoma. *Cancer Res* **54:** 1507–1510, 1994.
4. Cao S, Frank C, Shirasaka T and Rustum YM, 5-Fluorouracil prodrug: Role of anabolic and catabolic pathway modulation in therapy of colorectal cancer. *Clin Cancer Res* **1:** 839–845, 1995.
5. Cao S, Frank C and Rustum YM, Role of fluoropyrimidine schedule and (6R,S) leucovorin dose in a preclinical animal model of colorectal carcinoma. *J Natl Cancer Inst* **88:** 430–436, 1996.
6. Spector T, Porter DJT, Nelson DJ, Baccanari DP, Davis ST, Almond MR, Khor SP, Amyx H, Cao S and Rustum YM, 5-Ethynyluracil (776C85), a modulator of the therapeutic activity of 5-fluorouracil. *Drugs Future* **19:** 565–571, 1994.
7. Fischel JL, Etienne MC, Spector T, Formento P, Renee N and Milano G, Dihydropyrimidine dehydrogenase: A tumoral target for fluorouracil modulation. *Clin Cancer Res* **1:** 991–996, 1995.
8. Houghton JA and Houghton PJ, On the mechanism of cytotoxicity of fluorinated pyrimidines in four human colon xenografts maintained in immune-depressed mice. *Cancer* **45:** 1159–1167, 1980.
9. Wolberg WH and Morin J, Thymidylate synthetase activity and fluorouracil sensitivity of human colonic cancer and normal mucosal tissue preparations. *Cancer* **47:** 1313–1317, 1981.
10. Ishiwata K, Ido T, Abe Y, Matsuzawa T and Murakami M, Studies on ^{18}F-labeled pyrimidines III: Biochemical investigation of ^{18}F-labeled pyrimidines in comparison with ^{3}H-deoxythymidine in tumor-bearing rats and mice. *Eur J Nucl Med* **10:** 39–44, 1985.
11. Berne MHO, Gustavsson BG, Almersjo O, Spears PC and Frosing R, Sequential methotrexate/5-FU:FdUMP formation and TS inhibition in a transplantable rodent colon adenocarcinoma. *Cancer Chemother Pharmacol* **16:** 237–242, 1986.
12. Spears CP, Gustavsson BG, Berne M, Frosing R, Bernstein L and Hayes AA, Mechanisms of innate resistance to thymidylate synthase inhibition after 5-fluorouracil. *Cancer Res* **48:** 5894–5900, 1988.
13. El-Tahtawy A and Wolf W, *In vivo* measurements of intratumoral metabolism, modulation and pharmacokinetics of 5-fluorouracil, using ^{19}F nuclear magnetic resonance spectroscopy. *Cancer Res* **51:** 5806–5812, 1991.
14. Adams ER, Leffert JJ, Craig DJ, Spector T and Pizzorno G, *In vivo* effect of 5-ethynyluracil on 5-fluorouracil metabolism determined by ^{19}F nuclear magnetic resonance spectroscopy. *Cancer Res* **59:** 122–127, 1999.